

17. Schatz, J. F. & Simmons, G. Thermal conductivity of Earth materials at high temperatures. *J. Geophys. Res.* **77**, 6966–6983 (1972).
18. Holt, J. B. Thermal diffusivity of olivine. *Earth Planet. Sci. Lett.* **27**, 404–408 (1975).
19. Seipold, U. Temperature dependence of thermal transport properties of crystalline rocks—general law. *Tectonophysics* **291**, 161–171 (1998).
20. Hofmeister, A. M. Mantle values of thermal conductivity and the geotherm from phonon lifetimes. *Science* **283**, 1699–1706 (1999).
21. Klemens, P. G. Thermal conductivity and lattice vibrational modes. *Solid State Phys.* **7**, 1–98 (1958).
22. Bouhifid, M. A., Andrault, D., Fiquet, G. & Richet, P. Thermal expansion of forsterite up to the melting point. *Geophys. Res. Lett.* **23**, 134–136 (1996).
23. Vauchez, A., Barrool, G. & Tommasi, A. Why do continents break up parallel to ancient orogenic belts? *Terra Nova* **9**, 62–66 (1997).
24. Tommasi, A. & Vauchez, A. Continental rifting parallel to ancient collisional belts: An effect of the mechanical anisotropy of the lithospheric mantle. *Earth Planet. Sci. Lett.* **185**, 199–210 (2001).
25. Achauer, U. & KRISP working group. New ideas on the Kenya rift based on the inversion of the combined dataset of the 1985 and 1989/90 seismic tomography experiments. *Tectonophysics* **236**, 305–329 (1988).
26. Seipold, U. Simultaneous measurements of thermal diffusivity and thermal conductivity under high pressure using thermal pulse of finite length. *High Temp.-High Press.* **20**, 609–613 (1988).
27. Abramson, E. H., Brown, M., Slutsky, L. J. & Zaug, J. The elastic constants of San Carlos olivine up to 17 GPa. *J. Geophys. Res.* **102**, 12252–12263 (1997).
28. Duffy, T. S. & Vaughan, M. T. Elasticity of enstatite and its relationships to crystal structure. *J. Geophys. Res.* **93**, 383–391 (1988).

Acknowledgements

We thank C. Karger for participation in the measurements, and M. Ferrero and F. Boudier for providing the samples from Baldissero and Papua New Guinea, respectively. The Laboratoire de Tectonophysique's EBSD system was funded by the CNRS/INSU, Université de Montpellier II, and NSF project "Anatomy of an archaic craton". This work was supported by the CNRS/INSU programme "Action Thématique Innovante".

Correspondence should be addressed to A.T. (e-mail: deia@dstu.univ-montp2.fr).

Proteorhodopsin phototrophy in the ocean

Oded Béjà*†, Elena N. Spudich‡, John L. Spudich‡, Marion Leclerc* & Edward F. DeLong*

* Monterey Bay Aquarium Research Institute, Moss Landing, California 95039, USA

‡ Department of Microbiology and Molecular Genetics, The University of Texas Medical School, Houston, Texas 77030, USA

† These authors contributed equally to this work

Proteorhodopsin¹, a retinal-containing integral membrane protein that functions as a light-driven proton pump, was discovered in the genome of an uncultivated marine bacterium; however, the prevalence, expression and genetic variability of this protein in native marine microbial populations remain unknown. Here we report that photoactive proteorhodopsin is present in oceanic surface waters. We also provide evidence of an extensive family of globally distributed proteorhodopsin variants. The protein pigments comprising this rhodopsin family seem to be spectrally tuned to different habitats—absorbing light at different wavelengths in accordance with light available in the environment. Together, our data suggest that proteorhodopsin-based phototrophy is a globally significant oceanic microbial process.

Bacteriorhodopsin, a retinal-containing membrane protein that functions as a light-driven proton pump, was discovered nearly three decades ago in the halophile *Halobacterium salinarum*². The 'purple membranes' of this archaeon contain a high concentration of bacteriorhodopsin molecules, packed in an ordered two-dimensional crystalline array³. On absorption of light, bacteriorhodopsin undergoes a series of conformational shifts (a photocycle), causing a proton to be transported across the membrane. The resulting electrochemical membrane potential drives ATP synthesis, through

an H⁺-ATPase⁴. Similar rhodopsin-mediated, light-driven proton pumping, formerly thought to exist only in halophilic archaea, has been discovered in an uncultivated marine bacterium¹ of the 'SAR86' phylogenetic group⁵. This finding suggested that a previously unrecognized phototrophic pathway may occur in the ocean's photic zone; however, all earlier data are based solely on recombinant DNA and *in vitro* biochemical analyses, and this phenomenon has not yet been observed in the sea.

To test whether rhodopsin-like molecules form photoactive proteins in native marine bacteria, we analysed membrane preparations of bacterioplankton collected directly from Monterey Bay surface waters. Using laser flash-photolysis techniques⁶, we searched for spectroscopic evidence of proteorhodopsin-like photochemical activity in these bacterioplankton membrane preparations. We observed transient flash-induced absorption changes attributable to a photochemical reaction cycle of 15 ms (Fig. 1), which is characteristic of retinylidene ion pumps⁷ and similar to the photocycle seen with *Escherichia coli* membranes expressing recombinant proteorhodopsin¹.

Furthermore, 5 ms after the flash the absorption difference spectrum of the environmental sample exhibited the same shape and same isosbestic point for the light and dark state as proteorhodopsin expressed in *E. coli* membranes. This shows that photochemical reactions in native bacterioplankton cell membranes generate a red-shifted, long-lived intermediate spectrally similar to that of recombinantly expressed proteorhodopsin in *E. coli*. The flash-photolysis data provide direct physical evidence for the existence of proteorhodopsin-like transporters and endogenous retinal molecules in the microbial fraction of these coastal surface waters.

The photocycling pigment was bleached with hydroxylamine and, after hydroxylamine removal, photoactivity was restored by adding all-*trans* retinal (Fig. 2), showing that the photosignals do indeed derive from retinylidene pigmentation. We conclude that

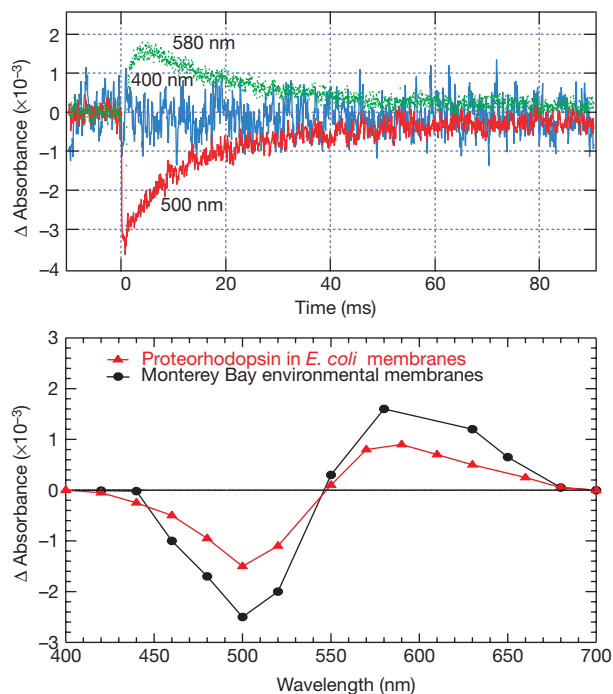


Figure 1 Laser flash-induced absorbance changes in suspensions of membranes prepared from the prokaryotic fraction of Monterey Bay surface waters. Top, membrane absorption was monitored at the indicated wavelengths and the flash was at time 0 at 532 nm. Bottom, absorption difference spectrum at 5 ms after the flash for the environmental sample (black) and for *E. coli*-expressed proteorhodopsin (red).

proteorhodopsin molecules are present in the membranes of native marine bacterioplankton.

The flash-photolysis data permit estimation of the cellular concentration of proteorhodopsin. Assuming (1) the flash yield of the environmental pigment is similar to that of proteorhodopsin expressed in *E. coli* (that is, 10.5% absorption change at 500 nm per absorption unit of pigment at 527 nm), we calculate 0.033 absorption units of proteorhodopsin at 527 nm (0.35 μg of proteorhodopsin protein per litre of sea water). Flash spectroscopy was necessary to detect the proteorhodopsin pigments because there is much greater absorption in the visible range by other pigments in the sample, which show peaks of 1.6, 1.3, 0.52 and 0.73 absorption units, at 437, 468, 647 and 673 nm, respectively.

Assuming also (2) a molar absorption coefficient of $50,000 \text{ M}^{-1} \text{ cm}^{-1}$ at the absorption maximum, (3) fluorescence *in situ* hybridization counts of a total of 5.6×10^{10} SAR86 cells in the concentrated sample (~10% of the total bacteria; see Methods), (4) 50% recovery of membranes from the cells, and (5) that the uncultivated SAR86 group is the principal bacterioplankton group using these pigments, we calculate that there are 2.4×10^4 proteorhodopsin molecules per SAR86 cell.

This value is on the order of the concentration of bacteriorhodopsin in a *H. salinarum* cell, in which substantial portions of the membrane surface area of the cell consist of bacteriorhodopsin in a tightly packed crystalline array⁸. For comparison, 2.4×10^4 bacteriorhodopsin molecules densely packed in the purple-membrane lattice would cover a 0.6- μm diameter, flat circular area of membrane—a significant portion of the surface of a single cell³. This number of molecules is sufficient to produce substantial amounts of ATP under illumination⁹. Therefore, the high density of proteorhodopsin in the SAR86 membrane indicated by our calculations strongly suggests that this protein has a significant role in the

physiology of these bacteria *in situ*.

To explore the possible existence of other proteorhodopsins, we screened the same mixed-population bacterial artificial chromosome (BAC) library¹⁰ in which proteorhodopsin was initially discovered, with non-degenerate polymerase chain reaction (PCR) primers¹. Several additional proteorhodopsin-containing BAC clones were found in the library. These proteorhodopsins were similar, but did differ in their amino-acid sequences when compared with the original proteorhodopsin (for example, see clones 31A8, 64A5 and 40E8; Figs 3 and 4). Using the same non-degenerate primers, we could also amplify by PCR proteorhodopsin genes from bacterioplankton DNA extracts, including those from Monterey Bay (MB clones; Fig. 3), the Southern ocean (Palmer station; PAL clones) and waters of the central North Pacific ocean (Hawaii Ocean Time series station¹¹; HOT clones).

We detected 15 different variants of proteorhodopsin in the PCR-generated Monterey Bay proteorhodopsin gene library, falling into three clusters (Fig. 3) that share at least 97% identity over 248 amino acids (Fig. 4) and 93% identity at the DNA level. Two proteorhodopsin genes from Monterey, 40E8 and 64A5, were expressed in *E. coli* and produced absorption spectra very similar to the original proteorhodopsin¹ (clone 31A8) isolated from the same waters (data not shown).

Remarkably, all the proteorhodopsin genes that were amplified by PCR from Antarctic marine bacterioplankton were different from those of Monterey Bay (Fig. 3), sharing a maximum of 78% identity over 248 amino acids with the Monterey clade (Fig. 4). The changes in amino-acid sequences were not restricted to the hydrophilic

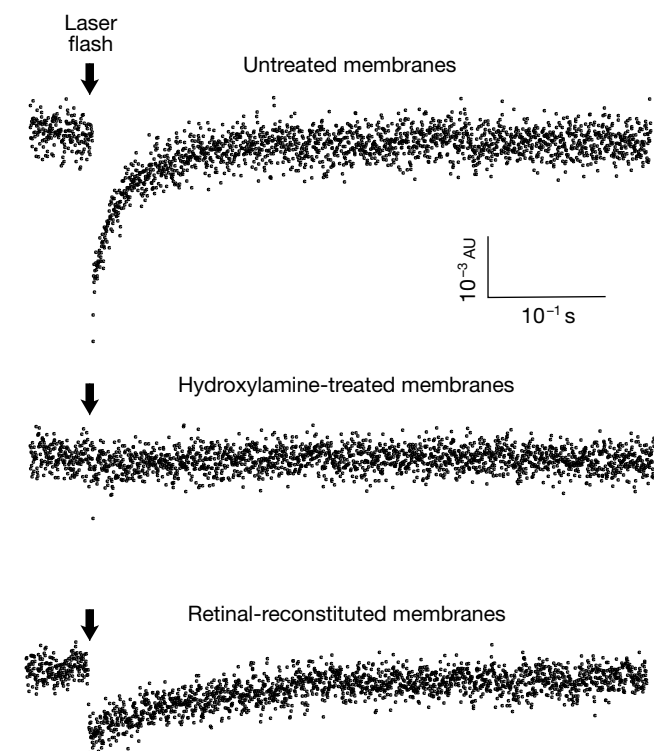


Figure 2 Laser flash-induced transients at 500 nm of a Monterey Bay bacterioplankton membrane preparation. Top, before addition of hydroxylamine; middle, after 0.2 M hydroxylamine treatment at pH 7.0, 18 °C, with 500-nm illumination for 30 min; bottom, after centrifuging twice with resuspension in 100 mM phosphate buffer, pH 7.0, followed by addition of 5 μM all-*trans* retinal and incubation for 1 h.

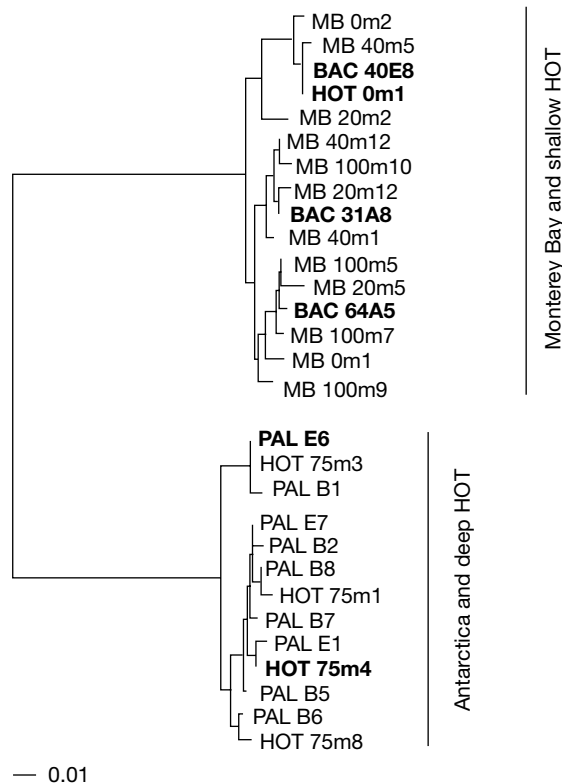


Figure 3 Phylogenetic analysis of the inferred amino-acid sequence of cloned proteorhodopsin genes. Distance analysis of 220 positions was used to calculate the tree by neighbour-joining using the PaupSearch program of the Wisconsin Package version 10.0 (Genetics Computer Group; Madison, Wisconsin). *H. salinarum* bacteriorhodopsin was used as an outgroup, and is not shown. Scale bar represents number of substitutions per site. Bold names indicate the proteorhodopsins that were spectrally characterized in this study.

loops but were spread over the entire protein, including changes near the retinal-binding domain (Fig. 4). Also, there was an insertion of one amino acid in the Antarctic proteorhodopsins, relative to those of the Monterey clade (Fig. 4).

We expressed the palE6 proteorhodopsin gene from Antarctica in *E. coli* cells. Addition of retinal to membranes of cells containing Antarctic proteorhodopsin apoprotein produced an absorbance peak at 490 nm (Fig. 5)—a blue shift of 37 nm from the 527-nm peak observed for the Monterey Bay proteorhodopsins. The Antarctic proteorhodopsin spectrum exhibited vibrational fine structure, as observed previously in retinylidene pigments for archaeal sensory rhodopsin II, which has a very similar blue-shifted (487-nm) absorption maximum¹². The nearly identical shapes of the structured spectra suggest similar mechanisms of wavelength regulation in the bacterial and archaeal rhodopsins. Furthermore, palE6 proteorhodopsin functions similarly to its Monterey Bay homologues¹, exhibiting light-mediated transport of protons in right-side-out *E. coli* vesicles (E. N. Spudich *et al.*, manuscript in preparation).

We screened a fosmid library from Antarctica (E. F. DeLong, unpublished data) with proteorhodopsin primers, and sequenced one clone containing the gene. Preliminary sequence analyses based on flanking gene order and identity indicate that, despite differences in amino-acid sequence and absorption spectra, the Antarctic proteorhodopsin is derived from a bacterium highly related to the proteorhodopsin-containing SAR86 bacteria of Monterey Bay¹⁰ (O. Béjà, unpublished data).

Thirty-two proteorhodopsin genes from the HOT station were cloned from surface (5-m) and 75-m samples. Most proteorhodopsin clones (80%) from the HOT surface waters belonged to the Monterey clade and were identical (on the amino-acid level) to the proteorhodopsin gene from BAC 40E8. In contrast, most of the clones from the 75-m sample (90%) fell within the Antarctic clade (Fig. 3). Two proteorhodopsin genes from the HOT station, HOT 0m1 and HOT 75m4, were expressed in *E. coli* and their absorption spectra were examined. As expected from their primary sequences, the HOT proteorhodopsin clustering with the Antarctic clade gave a blue (490-nm) absorption maximum, whereas the proteorhodopsin clustering with the Monterey clade gave a green (527-nm) absorption maximum (Fig. 5).

In the oligotrophic waters of the central North Pacific gyre, most of the light energy is in the blue range, with maximal intensity near 475 nm (ref. 13). This energy peak is maintained over depth, whereas the total energy decreases. At the surface, the energy peak is very broad with a half bandwidth between 400 and 650 nm. In deeper water below 50 m, the peak narrows and the half bandwidth is restricted to between 450 and 500 nm (Fig. 5). Considering the different wavelengths absorbed by members of the two different

proteorhodopsin clades (527 nm versus 490 nm; Fig. 5), it seems that the blue-shifted proteorhodopsin variants are better adapted to the light available in their environment. Notably, rod and cone visual pigment rhodopsins from closely related fish species in Lake Baikal¹⁴ also exhibit a blue shift in deeper dwelling species. In addition, previous studies of cultivated *Prochlorococcus*^{15,16} and *Synechococcus*¹⁷, as well as natural cyanobacterial communities¹⁸, also indicate the presence of surface- and deep-water groups adapted to different depths.

Our data now show the presence of co-existing surface- and deep-water clades of proteorhodopsin-based phototrophs, whose energy-generating pigments are spectrally tuned to either shallow or deeper water light fields. Presumably, this provides subsets of proteorhodopsin genetic variants in mixed populations with a selective advantage at different points along the depth-dependent light

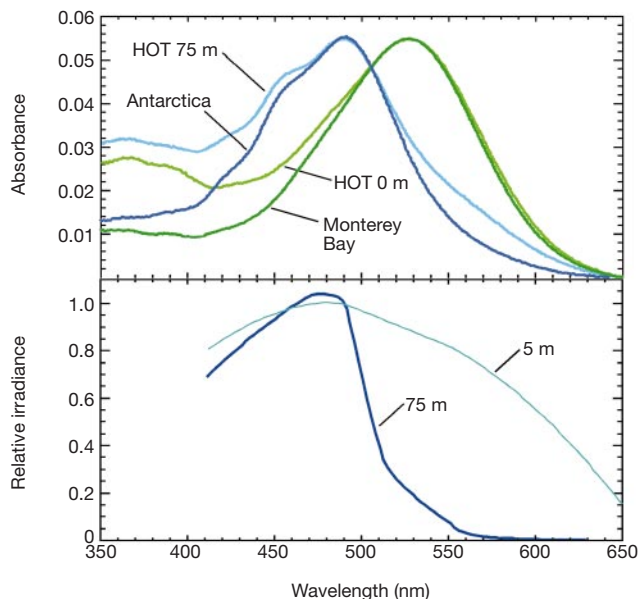


Figure 5 Absorption spectra of retinal-reconstituted proteorhodopsins in *E. coli* membranes. All-*trans* retinal (2.5 μ M) was added to membrane suspensions in 100 mM phosphate buffer, pH 7.0, and absorption spectra were recorded. Top, four spectra for palE6 (Antarctica), HOT 75m4, HOT 0m1, and BAC 31A8 (Monterey Bay) at 1 h after retinal addition. Bottom, downwelling irradiance from HOT station measured at six wavelengths (412, 443, 490, 510, 555 and 665 nm) and at two depths, for the same depths and date that the HOT samples were collected (0 and 75 m). Irradiance is plotted relative to irradiance at 490 nm.



Figure 4 Multiple alignment of proteorhodopsin amino-acid sequences. The secondary structure shown (boxes for transmembrane helices) is derived from hydropathy plots. Residues predicted to form the retinal-binding pocket are marked in red.

gradient. Of course, genetic variation other than proteorhodopsin tuning is likely to influence the fitness of population variants along the depth gradient. Other genetic loci may also co-vary with tuned absorption maxima, indicating a depth-optimized adaptation for these other traits as well. Genomic approaches should provide a means to test such hypotheses.

Proteorhodopsin-mediated phototrophic energy generation may have a significant impact on carbon and energy flux in the ocean. Although it is not known whether proteorhodopsin-bearing bacteria fix CO₂, their ability to generate energy from light should reduce overall respiratory energy requirements, as has been suggested for aerobic, bacteriochlorophyll-containing marine bacteria¹⁹. Bioenergetic calculations based on our data suggest that proteorhodopsin-based phototrophy could provide a large fraction of energy requirements for cell maintenance and reproduction. The widespread distribution and high abundance of SAR86 bacteria^{5,10,20–22}, combined with the biophysical and genetic data that we report, indicate that proteorhodopsin phototrophy is a biologically significant, globally distributed marine microbial process. □

Methods

Cell collection and membrane preparation

Antarctic coastal waters were collected off Palmer Station (64.4° S, 64.0° W), Anvers Island, Antarctic Peninsula, in August 1996 (ref. 23). Hawaiian HOT station (22.4° N, 158.0° W) waters were collected on 17 March 1998. Cell membranes were prepared from picoplankton cells concentrated from surface seawater (700l) collected in early winter 2000, roughly 26 miles offshore from Moss Landing, California (36.7° N, 122.4° W). Water samples were prefiltered through a GF/A glass-fibre filter (approximate particle size < 0.6 µm) to remove the larger eukaryotic phytoplankton cells. We concentrated the filtrate by tangential flow filtration¹⁹ and prepared the membranes²⁴ as described. Aliquots of the cell preparation were fixed in 3.7% formalin for subsequent fluorescence *in situ* hybridization and taxon-specific cell quantification.

Fluorescence *in situ* hybridization

BAC clones 31A08 and 27G05 (ref. 10) were used as templates to generate SAR86-specific polyribonucleotide probes targeted to large-subunit ribosomal RNA. We prepared fluorescently labelled polyribonucleotide probes that targeted a variable region of large subunit rRNA by *in vitro* transcription (M. Leclerc *et al.*, manuscript in preparation), and carried out subsequent whole-cell hybridization assays as described²⁵. The percentage of SAR86-type cells relative to total 4',6-diamidino-2-phenylindole dihydrochloride (DAPI)-stained cells was calculated as described²⁵.

Spectroscopy

One-half of the cell-membrane suspension (corresponding to 350l of seawater) was suspended in 2 ml of 100 mM sodium phosphate buffer, pH 7.0. Absorption spectra were measured on an Aminco DW2000 UV-visible absorption spectrophotometer (SLM; Urbana, IL). Flash-induced absorption transients in the millisecond to seconds time domain were acquired on a digital oscilloscope (Nicolet, Integra20) after a Nd-YAG laser flash (532 nm, 6-ns pulse duration, 40 mJ; Continuum, Surelight I) in a laboratory-constructed flash-photolysis system as described⁶. Each transient was obtained by averaging 64 acquisition sweeps collected at 30-s intervals at various wavelengths between 360 and 680 nm. We performed kinetic analyses with the program IGOR Pro, v3.1 (WaveMetrics, Lake Oswego, OR).

Received 3 January; accepted 26 March 2001.

1. Béjà, O. *et al.* Bacterial rhodopsin: evidence for a new type of phototrophy in the sea. *Science* **289**, 1902–1906 (2000).
2. Oesterheld, D. & Stoekenius, W. Rhodopsin-like protein from the purple membrane of *Halobacterium halobium*. *Nature* **233**, 149–152 (1971).
3. Henderson, R. & Unwin, P. N. Three-dimensional model of purple membrane obtained by electron microscopy. *Nature* **257**, 28–32 (1975).
4. Danon, A. & Stoekenius, W. Photophosphorylation in *Halobacterium halobium*. *Proc. Natl Acad. Sci. USA* **71**, 1234–1238 (1974).
5. Mullins, T. D., Britschgi, T. B., Krest, R. L. & Giovannoni, S. J. Genetic comparisons reveal the same unknown bacterial lineages in Atlantic and Pacific bacterioplankton communities. *Limnol. Oceanogr.* **40**, 148–158 (1995).
6. Sasaki, J. & Spudich, J. L. The transducer protein HtrII modulates the lifetimes of sensory rhodopsin II photointermediates. *Biophys. J.* **75**, 2435–2440 (1998).
7. Spudich, J. L., Yang, C. S., Jung, K. H. & Spudich, E. N. Retinylidene proteins: Structures and functions from archaea to humans. *Annu. Rev. Cell Dev. Biol.* **16**, 365–392 (2000).
8. Neugebauer, D. C., Zingsheim, H. P. & Oesterheld, D. Biogenesis of purple membrane in halobacteria. *Methods Enzymol.* **97**, 218–226 (1983).
9. Michel, H. & Oesterheld, D. Electrochemical proton gradient across the cell membrane of *Halobacterium halobium*: effect of N,N'-dicyclohexylcarbodiimide, relation to intracellular adenosine

- triphosphate, adenosine diphosphate, and phosphate concentration, and influence of the potassium gradient. *Biochemistry* **19**, 4607–4614 (1980).
10. Béjà, O. *et al.* Construction and analysis of bacterial artificial chromosome libraries from a marine microbial assemblage. *Environ. Microbiol.* **2**, 516–529 (2000).
11. Karl, D. M. & Lukas, R. The Hawaii Ocean Time-series (HOT) program: Background, rationale and field implementation. *Deep-Sea Res.* **43**, 129–156 (1996).
12. Takahashi, T. *et al.* Color regulation in the archaeobacterial phototaxis receptor phoborhodopsin (sensory rhodopsin II). *Biochemistry* **29**, 8467–8474 (1990).
13. Kirk, J. T. O. in *Light and Photosynthesis in Aquatic Ecosystems* 104–134 (Cambridge Univ. Press, Cambridge, 1983).
14. Bowmaker, J. K. The ecology of visual pigments. *Novartis Found. Symp.* **224**, 21–31 (1999).
15. Urbach, E., Scanlan, D. J., Distel, D. L., Waterbury, J. B. & Chisholm, S. W. Rapid diversification of marine picophytoplankton with dissimilar light-harvesting structures inferred from sequences of *Prochlorococcus* and *Synechococcus* (Cyanobacteria). *J. Mol. Evol.* **46**, 188–201 (1998).
16. Moore, L. R., Rocap, G. & Chisholm, S. W. Physiology and molecular phylogeny of coexisting *Prochlorococcus* ecotypes. *Nature* **393**, 464–467 (1998).
17. Palenik, B. Chromatic adaptation in marine *Synechococcus* strains. *Appl. Environ. Microbiol.* **67**, 991–994 (2001).
18. Ferris, M. J. & Palenik, B. Niche adaptation in ocean cyanobacteria. *Nature* **396**, 226–228 (1998).
19. Kolber, Z. S., Van Dover, C. L., Niderman, R. A. & Falkowski, P. G. Bacterial photosynthesis in surface waters of the open ocean. *Nature* **407**, 177–179 (2000).
20. Eilers, H., Pernthaler, J., Glockner, F. O. & Amann, R. Culturability and *in situ* abundance of pelagic bacteria from the North Sea. *Appl. Environ. Microbiol.* **66**, 3044–3051 (2000).
21. Gonzalez, J. M. *et al.* Bacterial community structure associated with a dimethylsulfoniopropionate-producing North Atlantic algal bloom. *Appl. Environ. Microbiol.* **66**, 4237–4246 (2000).
22. Rappé, M. S., Vergin, K. & Giovannoni, S. J. Phylogenetic comparisons of a coastal bacterioplankton community with its counterparts in open ocean and freshwater systems. *FEMS Microbiol. Ecol.* **33**, 219–232 (2000).
23. DeLong, E. F. *et al.* Dibiphytanyl ether lipids in nonthermophilic crenarchaeotes. *Appl. Environ. Microbiol.* **64**, 1133–1138 (1998).
24. Shimono, K., Iwamoto, M., Sumi, M. & Kamo, N. Functional expression of pharaonis phoborhodopsin in *Escherichia coli*. *FEBS Lett.* **420**, 54–56 (1997).
25. DeLong, E. F., Taylor, L. T., Marsh, T. L. & Preston, C. M. Visualization and enumeration of marine planktonic archaea and bacteria by using polyribonucleotide probes and fluorescent *in situ* hybridization. *Appl. Environ. Microbiol.* **65**, 5554–5563 (1999).

Acknowledgements

We thank J. Zehr and D. Karl for the HOT samples and the captain and crew of the RV *Point Lobos* for expert assistance at sea. D. Karl and R. Letellier provided spectral irradiance data. This research was supported by the National Science Foundation (E.F.D.), the NIH (J.L.S.), and the David and Lucile Packard Foundation (E.F.D.).

Correspondence and requests for materials should be addressed to E.F.D. (e-mail: delong@mbari.org). The sequences have been deposited with GenBank under accession numbers AF349976–AF350003.

Large-scale forest girdling shows that current photosynthesis drives soil respiration

Peter Högberg*, **Anders Nordgren***, **Nina Buchmann†**, **Andrew F. S. Taylor‡**, **Alf Ekblad*§**, **Mona N. Högberg***, **Gert Nyberg***, **Mikael Ottosson-Löfvenius*** & **David J. Read||**

* *Section of Soil Science, Department of Forest Ecology, SLU, SE-901 83 Umeå, Sweden*

† *Max-Planck Institute for Biogeochemistry, PO Box 100164, 07701 Jena, Germany*

‡ *Department of Forest Mycology and Pathology, SLU, PO Box 7026, SE-750 07 Uppsala, Sweden*

|| *Department of Animal and Plant Sciences, University of Sheffield, Sheffield S10 2TN, UK*

The respiratory activities of plant roots, of their mycorrhizal fungi and of the free-living microbial heterotrophs (decomposers) in soils are significant components of the global carbon balance, but their relative contributions remain uncertain^{1,2}. To separate mycorrhizal root respiration from heterotrophic respiration in a

§ Present address: Department of Natural Sciences, Örebro University, SE-701 82 Örebro, Sweden.